Title: A meta-analysis of the stony coral tissue loss disease microbiome finds key bacteria in lesions and unaffected tissue of diseased colonies

Running title: SCTLD microbiome meta-analysis

Stephanie M. Rosales[1,2], Lindsay K. Huebner[3], James S. Evans[4], Amy Apprill[5], Andrew C. Baker[6], Anthony J. Bellantuono[7], Marilyn E. Brandt[8], Abigail S. Clark[9], Javier del Campo[10], Caroline E. Dennison[6], Naomi E. Huntley[11], Christina A. Kellogg[4], Mónica Medina[11], Julie L. Meyer[12], Erinn M. Muller[13], Mauricio Rodriguez-Lanetty[7], Jennifer L. Salerno[14], William B. Schill[15], Erin N. Shilling[16], Julia Marie Stewart[11], Joshua D. Voss[16]

1. Cooperative Institute for Marine and Atmospheric Studies, Miami, FL, United States
2. Atlantic Oceanographic and Meteorological Laboratory, Miami, FL, United States
3. Florida Fish and Wildlife Conservation Commission, Fish and Wildlife Research Institute, St. Petersburg, FL, USA
4. U.S. Geological Survey, St. Petersburg Coastal and Marine Science Center, St. Petersburg, FL, USA
5. Woods Hole Oceanographic Institution, Marine Chemistry and Geochemistry, Woods Hole, MA USA
6. The University of Miami, Rosenstiel School of Marine, Atmospheric, and Earth Science, Department of Marine Biology and Ecology, Miami, FL, USA
7. Florida International University, Department of Biological Sciences, Miami, FL, USA
8. The University of the Virgin Islands, Center for Marine and Environmental Studies, St. Thomas, VI, U.S. Virgin Islands
9. The College of the Florida Keys, Marine Science and Technology, Key West, FL, USA
10. Institut de Biologia Evolutiva (CSIC - Universitat Pompeu Fabra)-Barcelona, Spain
11. The Pennsylvania State University, Biology Department, University Park, PA, USA
12. The University of Florida, Soil, Water, and Ecosystem Sciences Department, Gainesville, FL, USA
13. Mote Marine Laboratory, Coral Health and Disease Program, Sarasota, FL, USA
14. George Mason University, Potomac Environmental Research and Education Center, Department of Environmental Science and Policy, Woodbridge, VA, USA
15. U.S. Geological Survey, Eastern Ecological Science Center, Leetown, WV, USA
16. Harbor Branch Oceanographic Institute, Florida Atlantic University, Fort Pierce, FL, USA

Abstract

Stony coral tissue loss disease (SCTLD) has been causing significant whole colony mortality on reefs in Florida and the Caribbean. The cause of SCTLD remains unknown, with limited concurrence of SCTLD-associated bacteria among studies. We conducted a meta-analysis of SSU 16S ribosomal RNA gene datasets generated by 16 field and laboratory SCTLD studies to find consistent bacteria associated with SCTLD across disease zones (vulnerable, endemic, and epidemic), coral species, coral compartments (mucus, tissue, and skeleton), and disease states (apparently healthy colony tissue [AH], and unaffected [DU] and lesion [DL] tissue from diseased colonies). We also evaluated bacteria in seawater and sediment, which may be sources of SCTLD transmission. Although AH colonies in endemic and epidemic zones harbor bacteria associated with SCTLD lesions, and aquaria and field samples had distinct microbial compositions, there were still clear differences in the microbial composition among AH, DU, and DL in the combined dataset. Alpha diversity between AH and DL was not different; however, DU showed increased alpha diversity compared to AH, indicating that, prior to lesion formation, corals may undergo a disturbance to the microbiome. This disturbance may be driven by Flavobacteriales, which were especially enriched in DU. While Rhodobacterales and Peptostreptococcales-Tissierellales were prominent in structuring microbial interactions in DL. Peptostreptococcales-Tissierellales specifically may contribute to lesion progression through an alpha-toxin. We provide a consensus of SCTLD-associated bacteria both prior to and during lesion progression and identify how

these taxa vary across studies, coral species, coral compartments, seawater, and sediment.

Keywords: SCTLD, Peptostreptococcales-Tissierellales, Rhodobacterales, Flavobacteriales, coral disease, Florida, U.S. Virgin Islands

Introduction

Stony coral tissue loss disease (SCTLD) causes focal or multifocal lesions on hard coral colonies (order Scleractinia) leading to exposed skeleton from tissue loss [1, 2]. Affected colony mortality rates can be as high as 99%, but survival is highly dependent on the coral species [3]. While some corals, such as branching Caribbean acroporids, are not impacted by this disease [3], SCTLD nevertheless has a wide host range, affecting over half of Caribbean coral species (~22 species) [2, 3]. This has resulted in a decline in coral species richness, coral cover, and ecosystem function throughout Florida and the Caribbean [3–10].

The cause of SCTLD is currently unknown, but multiple hypotheses of the potential etiology have been proposed, including abiotic stressors [3, 4, 11, 12], viruses [13, 14], bacteria [15, 16], or a combination. SCTLD was first detected in September 2014 off the coast of Miami, Florida, coincident with a dredging project to expand the Miami Port and a coral bleaching event [3, 4]. This led to speculation that heat stress and/or sedimentation may be linked to SCTLD. Evidence to date suggests that thermal stress

has either no association with SCTLD [17] or slows disease progression [18], but sediments may contribute to SCTLD transmission [11, 12].

SCTLD is contagious and can be transmitted through the water column [18–20] or through direct coral-coral contact [21], suggesting that it is caused by a biotic source(s) [9, 22]. Viruses have been found in SCTLD-affected corals, although similar virus morphologies and sequences were also detected in apparently healthy corals at similar abundances [13, 14]. Studies have also detected ciliates [1, 22, 23] and endolithic organisms [24] associated with SCTLD, but other eukaryotes have not been associated with this disease.

The most well-studied SCTLD microbial group is the bacterial community, examined using small subunit (SSU)16S rRNA gene analysis [11, 12, 15, 16, 23, 25–29]. It is likely that the bacterial community is important for SCTLD progression, since there is a shift in bacterial composition from healthy corals to diseased corals, and SCTLD lesion progression can be mitigated using antibiotics [22, 30, 31]. Orders such as Rhodobacterales, Rhizobiales, Clostridiales, Alteromonadales, and Vibrionales have been described across many studies, but there have been discrepancies, especially at finer taxonomic levels. Further, a consensus on the key bacteria associated with SCTLD across locations and coral species remains a topic of discussion.

The lack of consensus across studies may be due to biological factors such as coral species-specific microbiomes, the environment in which samples were collected, or

other biological variables. However, variability across studies may also arise from different laboratory processing, library preparation, and analytical approaches [32]. In addition, results are often reported at different taxonomic levels such as order [11], family [16], genus [15], and species [25], which can make it difficult to compare across studies. Thus, to better understand SCTLD, a meta-analysis of available SSU 16S rRNA datasets can reduce biases associated with pipelines and reporting strategies. In this study, we examined microbiome datasets from 16 SCTLD studies using a consistent analysis pipeline to determine global patterns and taxa associated with SCTLD.

Results

Summary of SCTLD microbiome studies

Initially, datasets were acquired from 17 SCTLD studies, but one study [26] did not pass quality filtering and was removed from the analysis, resulting in 16 SCTLD studies used in this meta-analysis. Additionally, one *Acropora* spp. rapid tissue loss (RTL) disease study was included for comparison of bacteria which may be associated more generally with coral tissue loss diseases (Supplemental Table 1). The combined dataset included 2,425 samples, representing various coral species and environments described below. After the removal of miscellaneous samples such as lab controls, 2,362 samples remained (Supplemental Table 1). Samples from the studies were sequenced using five primer pairs: CS1-515F/CS2-806R [33] with additional 5' linker sequences [34] (n=79),

515FY [35]/806RB [36] (n=1,219), S-D-Bact-0341-b-S-17/S-D-Bact-0785-a-A-21 [37] (n=31), 515F/806R [33] (n=49), and 515F [33]/Arch806R [38] (n=984; Figure 1A).

Samples were collected throughout Florida and the U.S. Virgin Islands (USVI). Field samples totaled 1,274, representing 40 sites, and a further 1,088 samples were from aquaria (i.e., laboratory-based experiments; Figure 1). Thirteen SCTLD-susceptible coral species were included, with *Montastraea cavernosa* (MCAV; n=543) and *Orbicella faveolata* (OFAV; n=357) most represented and *Pseudodiploria clivosa* (PCLI; n=6) and *Orbicella franksi* (OFRA; n=7) least represented (Figure 1). Coral samples (n=2,031) were from three compartments: mucus only (n=393), mucus and surface tissue (tissue slurry; n=1,585), and skeleton samples with embedded coral tissue (tissue slurry skeleton; n=53). Seawater (n=198) and sediment (n=133) samples from both the field and aquaria experiments also were included (Figure 1B). Coral samples represented three SCTLD health states: apparently healthy colonies (AH), which was the most represented (n=1,021), followed by lesions on diseased colonies (DL; n=661), and unaffected areas on diseased colonies (DU; n=349; Figure 1C).

Differences in the microbial composition were found among zones (vulnerable, endemic, and epidemic)

For alpha diversity for AH field-sourced samples, after filtering, 41,504 amplicon sequence variants (ASVs) remained, which were reduced to 15,021 following rarefaction. Among AH samples, there was a slight decrease in Shannon (alpha)

diversity from the vulnerable zone (estimated marginal means [emmean]=3.95) to the epidemic zone (emmean=3.70), but this was not significant (Supplemental Fig. 1). For beta diversity, the dispersion was also not different between zones. A PERMANOVA pairwise comparison was significant for all comparisons between zones (p-adjusted [padj] <0.03; Figure 2A), which was adjusted by location given that epidemic samples from the USVI clustered separately from Florida epidemic samples. Differential abundance analysis found 61 ASVs enriched between vulnerable and endemic sites (Figure 2B and Supplemental Table 2). In the endemic zone, the orders Synechococcales (*Cyanobium* PCC-6307; log-fold=12.67) and an uncultured Flavobacteriales (log-fold=9.96) contained ASVs with the highest log-fold change, but the order Flavobacteriales was the group of bacteria with the most enriched ASVs (n=13), followed by SAR11 clade (n=4) and Rhodobacterales (n=3). Fewer ASVs were enriched between the vulnerable and epidemic zones (n=31; Figure 2C and Supplemental Table 3), with the highest log-fold ASV changes found in the orders Burkholderiales (*Delftia*; log-fold=5.84) and Peptostreptococcales-Tissierellales (*Fusibacter*; log-fold=5.65). Like in endemic sites, Flavobacteriales was the group with the most enriched ASVs in the epidemic zone (n=5).

Disease state showed the lowest correlation to beta diversity

Microbial dispersion was found to be different across primers, study, biome, year, all coral species, and sample type (Permutest: $p<0.01$; Figure 3). A PERMANOVA test for differences between microbial composition was also significant across all factors, with

coral species having the highest correlation (R^2=0.21; Figure 3E) and disease state showing the lowest correlation (R^2=0.04).

Differences found between aquaria and field samples based on disease state

Biome (i.e., aquaria and field) had the largest correlation to principal component 1 (PC1, R^2=0.73; Supplemental Fig. 2) than other tested metadata factors, and showed a distinct separation when visualized (Figure 3C). This was also evident even in sediment and seawater samples that were collected in aquaria studies, which clustered with coral samples from aquaria studies and not with field sediment and seawater samples. Given this pattern, SCTLD-affected corals (with the removal of *Acropora* spp.) were first analyzed combined (i.e., both aquaria and field) and then subsequent analysis was divided by biome to identify potential differences between the two. When both biomes were combined (Figure 4A), AH microbial communities were the most highly dispersed compared to both DU (padj<0.01) and DL (padj<0.02), but DU vs DL were not different. Pairwise PERMANOVA was significant for all comparisons (padj<0.03 each): AH vs DU (R^2=0.07), AH vs DL (R^2=0.03), and DU vs DL (R^2=0.13; Figure 4A). Among aquaria samples (Figure 4B), the dispersion was lower in DU vs both DL and AH (padj<0.0001 each) but was similar in AH vs DL. Like the combined samples, all aquaria samples were different in the pairwise PERMANOVA (R^2=0.03, padj<0.03 each; Figure 4B). In field samples (Figure 4C), dispersion was lowest in DL compared to both AH and DU (padj<0.0001 each) but there was no difference between DU vs DL. All pairwise PERMANOVA comparisons were significant in the field samples: AH vs DU (R^2=0.01,

padj<0.03), AH vs DL (R^2=0.03, padj<0.01), and DU vs DL (R^2=0.08, padj<0.03; Figure 4C).

Samples were also evaluated for alpha diversity by disease state in each biome. After quality filtering and rarefaction across disease states, 39,513 ASVs remained. For aquaria and field samples combined, pairwise comparisons showed differences in Shannon diversity for AH vs DU and DL vs DU (padj<0.0001 each) but not AH vs DL, with mean alpha diversity lowest in DL (emmean=3.42) and highest in DU (emmean=3.85; Supplemental Fig. 3A). In aquaria samples only, there were no differences in Shannon diversity by disease state, likely due to the low sample size of DU (n=27, Supplemental Fig. 3B). In field samples, only DU vs DL was different (padj<0.01) with DU also showing the highest mean (emmean=3.90) and DL the lowest (emmean=3.63; Supplemental Fig. 3C) alpha diversity.

When comparing differences in mean relative microbial abundances within disease states across biomes, AH samples differed between aquaria and field (Supplemental Fig. 3D): the orders Rhodobacterales (14.20±5.2%) and Cytophagales (9.02±12.32%) were dominant in aquaria samples, but in field samples, the dominant orders were Flavobacteriales (5.75±2.15%) and Synechococcales (3.77±5.88%). Like AH aquaria samples, DU aquaria samples had the highest mean relative abundances in Rhodobacterales, but at a much lower percentage (1.06±3.81%). The DU field samples were also similar to their AH counterparts, showing the highest relative abundances in Flavobacteriales (6.43±1.89%) and Synechococcales (4.45±6.26%). In the DL samples,

both aquaria and field samples were dominated by Rhodobacterales, but the aquaria samples had a higher relative abundance of Rhodobacterales (15.34±6.84%) than samples from the field (6.61±4.12%). As with aquaria AH samples, Cytophagales (3.28±11.22%) were also the second most relatively abundant order in DL aquaria samples but were not dominant in field DL samples. Peptostreptococcales-Tissierellales was a dominant DL member at similar mean relative abundances in both aquaria (3.21±6.40%) and field samples (3.79±9.06%; Supplemental Fig. 3D).

Indicator taxa were detected across coral compartments, seawater, and sediment

The combined three coral compartments (mucus, tissue slurry, and tissue slurry skeleton), from both field and aquaria, yielded a total of 109 differentially abundant ASVs between AH vs DU (Figure 5A and Supplemental Table 4). DU mucus samples showed the highest log fold change compared to AH in the orders Flavobacteriales (NS5 marine group; log-fold=6.33) and Synechococcales (*Cyanobium* PCC-6307; log-fold=6.19), with Flavobacteriales having the most enriched ASVs (n=9). Similarly, DU tissue slurry samples were most enriched in Synechococcales (*Synechococcus* CC9902; log-fold=20.04) and Flavobacteriales (NS5 marine group; log-fold=12.71), with Flavobacteriales having the most enriched ASVs (n=9). Tissue slurry skeleton sample comparisons of AH vs DU identified no ASVs enriched in DU. In addition to coral compartment samples, ASVs enriched in AH and DU samples were also present within sediment and seawater samples (Figure 5B).

When OFAV and MCAV (the most-sampled coral species) were removed from the analysis, similar patterns were still identified in beta diversity and differential abundance when compared to the analysis of all SCTLD-susceptible species (Supplemental Fig. 4A and B). For DU, 18 (35.3%) ASVs were shared between the two analyses (i.e., with vs without OFAV and MCAV), but more unique ASVs were found enriched in the analysis without OFAV and MCAV compared to the analysis that included all SCTLD-susceptible corals. Still, the two analyses shared more enriched bacterial families compared to the number that was enriched only within each individual analysis.

The three combined coral compartments yielded fewer differentially abundant ASVs in AH vs DL (n=79; Figure 6A and Supplemental Table 5) compared to AH vs DU (Figure 5A). In DL mucus samples, ASVs from the orders Desulfovibrionales (*Halodesulfovibrio*; log-fold=13.96) and Rhodobacterales (*Shimia*; log-fold=13.18) were the most enriched, and Rhodobacterales had the most enriched ASVs overall (n=8). In DL tissue slurries, the ASVs with the highest enrichment were two Rhodobacterales from an uncharacterized genus (log-fold=15.77) and one from the genus *Tropicibacter* (log-fold=13.46). Rhodobacterales was also the order with the most enriched ASVs in DL compared with AH tissue slurries (n=14), followed by Peptostreptococcales-Tissierellales (n=6). Among tissue slurry skeleton samples, only one ASV was enriched in DL (Burkholderiales, *Achromobacter*; log-fold=1.49). ASVs enriched in DL were also found in sediment and seawater (Figure 6B). In DL, the differential abundance analysis without OFAV and MCAV compared to that with all SCTLD-susceptible coral species

261 showed that the majority of enriched ASVs were shared (n=25; 39.1%) between the two
262 analyses (Supplemental Fig. 4C).
263
264 ***The presence of indicator taxa varied across coral species and studies***
265
266 Six coral species were represented by a high number of samples (n>76 samples each),
267 and all ASVs only enriched in DU were found within all of those species. The seven
268 coral species with lower sampling frequencies (n<76 each) varied in the numbers of DU-
269 enriched ASVs present (Supplemental Fig. 5A). For example, *Dichocoenia stokesii*
270 (DSTO) contained all DU-enriched taxa, and *Stephanocoenia intersepta* (SINT) had all
271 genera present but one, which belonged to Flavobacteriales. In comparison,
272 *Pseudodiploria clivosa* (PCLI) had the fewest DU-enriched taxa (n=3) among the coral
273 species. Four orders were not present in *Acropora* spp. samples and included:
274 Blastocatellales, Pirellulales, Sphingobacteriales, and Peptostreptococcales-
275 Tissierellales. Across studies, the order Sphingobacteriales was not found in any
276 aquaria study but was found in 50% of field studies (Supplemental Fig. 5B). Additionally,
277 no aquaria study had representatives from all DU-enriched taxa, but four field studies
278 were found to have all taxa. The two studies with the fewest representatives were
279 studies that used V3-V4 primers (Supplemental Table 1).
280
281 The ASVs enriched only in DL were also present in all high-frequency coral species,
282 while none of the low-frequency coral species had all of the DL-enriched taxa
283 (Supplemental Fig. 6A). PCLI possessed the fewest DL-enriched genera (n=9) followed

by *Orbicella franksi* (OFRA; n=15). More DL-enriched orders (n=11) were absent from *Acropora* spp. Corals (n=4) than DU-enriched orders; the DL orders not present in *Acropora* were: Bacteroidales, Beggiatoales, Burkholderiales, Cellvibrionales, Clostridiales, Desulfovibrionales, Oligoflexales, Peptostreptococcales-Tissierellales, Rhizobiales, Thiotrichales, and Verrucomicrobiales. Across studies, three had all the DL-enriched orders (all aquaria studies), and the fewest orders were present in those which used V3-V4 primers (Supplemental Fig. 6B), as with the DU-enriched orders.

Alphaproteobacteria and Clostridia were found as important players in SCTLD bacterial community interactions

In a network analysis of co-associated ASVs, a total of nine modules were identified, with two that were significantly and positively correlated to AH (R^2=0.26 and 0.1), three to DU (R^2=0.12, 0.31, and 0.46), and four to DL (R^2=0.17, 0.22, 0.46, and 0.47; Supplemental Fig. 7). The modules with the highest positive correlation to each disease state had 134 (AH; blue), 158 (DU; green), and 146 (DL; pink) co-abundant ASVs (Supplemental Fig. 7) and were used for undirected network analysis (Figure 7). Although AH had the second largest module, the network was smaller than both DU and DL, with only 56 ASV nodes and 59 edges (connections between nodes). DU had the largest network, with 138 nodes and 293 edges, followed by DL, with 123 nodes and 204 edges. In AH, the node with the most neighbors (n=7) was from the class Polyangia (order Polyangiales), which was also considered in the AH network to be a key player (i.e., provides cohesiveness, connectedness, and is embedded in a network; Figure 7).

The two nodes with the highest correlation to the blue weighted correlation network analysis (WGCNA) module (Supplemental Fig. 7) were from the class Bacteroidia (Chitinophagales; R^2=0.88 and 0.87).

In the DU network, highly connected nodes included three Alphaproteobacteria (SAR11 clade [n=16], Rhodobacterales [n=11], and Rhodospirillales [n=11]; Figure 7). Alphaproteobacteria were among the classes assigned as key players, but additional key players included: Cyanobacteria, Bacteroidia, and Polyangia. The nodes most highly correlated to their respective WGCNA modules were SAR86 clade (R^2=0.88) and Rhodospirillales (R^2=0.88).

The DL network had nodes with the most neighbors compared to AH and DU and was driven by Alphaproteobacteria (two Rhodobacterales nodes [n=22 and n=16], and Rhizobiales [n=9]), and Bacteroidia (Flavobacteriales [n=12]; Figure 7). While Alphaproteobacteria (Rhodobacterales and Rhizobiales) were found as key players in DL, Flavobacteriales were not. Additional key players in DL included Clostridia, Chlamydiae, and Campylobacteria. The class Clostridia had the highest correlations to the DL pink WGCNA module (Peptostreptococcales-Tissierellales; R^2=0.77 and Lachnospirales R^2=0.76; Supplemental Fig. 7). The most prevalent classes in DL networks were Alphaproteobacteria (n=39; mainly Rhodobacterales, n=29) and Clostridia (n=23; mainly Peptostreptococcales-Tissierellales, n=13).

The top microbial functional pathways were more enriched in DL compared to AH and DU

To identify differences in the potential microbial function between disease states, we used the SSU16S rRNA gene for functional predictions. There was a total of 6,307 differently abundant (padj<0.05) Kyoto Encyclopedia of Genes and Genomes (KEGG) pathways identified across AH (n=2,482), DU (n=1,403), and DL (n=2,422). Of the top 10 KEGG pathways, three were enriched in DU and six in DL (Supplemental Fig. 8A). The most enriched pathway in DU was 4-hydroxybutyrate dehydrogenase (effect size=0.25), and in DL was phospholipase C/alpha-toxin (effect size=0.97). A total of 392 differentially abundant MetaCyc pathways were found across AH (n=148), DU (n=104), and DL (n=139). Out of the top 10 pathways, nine were enriched in DL and one in DU (Supplemental Fig. 8B). Biotin biosynthesis II was the most enriched pathway in DL (effect size=0.80), and ADP-L-glycero-β-D-manno-heptose biosynthesis in DU (effect size=0.05).

Discussion

We used a crowdsourcing approach of both unpublished and published data to better understand stony coral tissue loss disease (SCTLD) across zones of disease spread (vulnerable, endemic, and epidemic), coral species, biomes (field vs aquaria), and studies to provide a more informed consensus on SCTLD-associated bacteria. We identified potential changes to coral microbiomes based on the length of time the disease had been present in the area (i.e., epidemic vs endemic zones). We also found

differences in alpha and beta diversity by coral disease state: apparently healthy colonies (AH), and unaffected areas (DU) and lesions (DL) on diseased colonies. Furthermore, DU and DL showed unique sets of enriched bacteria, with DL microbiomes particularly structured by Rhodobacterales and Peptostreptococcales-Tissierellales interactions.

Apparently healthy field-sourced coral microbiome composition differed among SCTLD zones

To understand if SCTLD alters the microbiome of visibly healthy corals on SCTLD-affected reefs, we examined AH corals within three disease zones: vulnerable, epidemic, and endemic. Although there were no differences in alpha diversity and dispersion among zones, microbial beta diversity and enriched microbial taxa were different among zones, as previously documented [11]. AH corals in the endemic and epidemic zones harbored SCTLD-associated microbes such as Alteromonadales, Vibrionales, Peptostreptococcales-Tissierellales, and Rhodobacterales, potentially indicating they were actively combating or showing signs of resistance to the disease. Flavobacteriales was the group with the most enriched taxa in endemic and epidemic AH corals, which is notable because Flavobacteriales were also detected in both DU and DL and are known to associate with corals under stressful conditions [39]. As AH corals showed no outward signs of lesions, members of Flavobacteriales may represent initial members of the SCTLD microbiome. However, a better understanding of the specific species or strains of Flavobacteriales present in both healthy and diseased

corals may explain their enrichment in different health states as Flavobacteriales was also found at high abundances in AH.

SCTLD aquaria studies may change microbial dynamics compared to field studies

We found that both biomes (aquaria and field) had distinct microbial compositions, which has been reported previously [40]. Despite this, we detected a microbial composition shift in disease states in both biomes, but field samples had a stronger beta diversity correlation in AH vs DL comparisons. Furthermore, there were notable differences in the relative abundances of certain taxa between biomes. For example, while Rhodobacterales were dominant members in both biomes, they were found at higher relative abundances in aquaria compared to field samples. Because Rhodobacterales are primary surface colonizers in marine waters, including surfaces such as glass [41] aquarium environments may provide conditions that particularly enrich Rhodobacterales over other bacterial taxa. Additionally, aquaria showed high relative abundances of Cytophagales in AH and DL, but this taxon was not a top abundant order in field samples. An aquaria coral challenge study with *Vibrio coralliilyticus* also showed an enrichment of both Rhodobacterales and Cytophagales [42], further indicating that aquarium conditions may select for these two taxa. Interestingly, Peptostreptococcales-Tissierellales, a bacterial group that appears to be important within SCTLD lesions, was present at similar relative abundances in DL in

both biomes and thus may be less susceptible to laboratory artifacts than Rhodobacterales.

Notably, there were two aquaria experiments designed to limit the 'microbial background noise' from the field by using sterilized seawater [29] or sterilized sediment [12] and then incubating the chosen medium with healthy or diseased corals. The resulting bacterial communities from the incubated seawater and sediment clustered with aquaria coral samples rather than with field seawater and sediment samples, and show that these inoculums likely take on the host microbial community. While field sediment and seawater samples showed distinct community separation from field coral samples, these samples still showed enrichment of some ASVs found in field DU and DL tissues, indicating potential transfer of microbes between diseased corals and their environment, which may result in continued transmission of SCTLD [11].

Unaffected tissues on diseased colonies were enriched with Flavobacteriales and Synechococcales

This meta-analysis provides a comprehensive list of important microbial taxa in SCTLD across three coral compartments (mucus, tissue slurry, and tissue slurry skeleton) and three disease states (AH, DU, DL). DU areas on coral colonies are of interest as they may represent an initial disturbance from SCTLD to the microbial community with potentially fewer secondary and saprophytic bacteria. It is unknown if SCTLD is a localized or systemic condition, but histological studies have found internal SCTLD

lesions in DU tissue prior to lesion formation on the colony surface [21, 24]. We found that DU samples had the highest alpha diversity and a distinct microbial composition, further suggesting that SCTLD also causes disruptions in the microbiome prior to surface lesion formation. Compared to AH, DU becomes particularly enriched with Flavobacteriales (class Bacteroidia) and Synechococcales (class Cyanophyceae), and these taxa formed strong connections to the class Alphaproteobacteria from the orders SAR11 and Rhodobacterales. However, SAR11 interactions may only be important in the mucus, which was the only compartment in which they were enriched.

Of note, the increase in DU alpha diversity could be partly driven by the lack of standardization of DU samples. One study collected DU samples from colonies in which DL tissues were treated with antibiotics, potentially disrupting the DU microbiome [43]. The remaining studies consistently sampled DL at the lesion margin, but the DU samples varied in distance collected from the lesion. This may be driving the diversity detected, as the DU microbial community is known to change with distance from the lesion, with samples closest to the lesion possessing more SCTLD-associated taxa than those farther away [15]. A standardized definition of DU should be employed to maximize the utility of these samples. Regardless, the majority of DU-enriched taxa are likely not primary pathogens, as they were also found in the *Acropora* spp. rapid tissue loss (RTL) study. However, one Blastocatellales and Peptostreptococcales-Tissierellales ASV each were not found in the RTL study but were prevalent in 73% of the SCTLD studies, and therefore could be specific to SCTLD. Although these two ASVs have a 100% sequence similarity to bacteria found within black band disease

(accession MH341639; [44]), and a paling necrosis study (GU200211.1; [43]), respectively, the studies took place outside of the Caribbean and thus the ASVs could belong to bacteria newly introduced to the area.

Rhodobacterales and Peptostreptococcales-Tissierellales were key structural components of microbial interactions in disease lesions

There was no clear transition from AH to DU to DL in alpha diversity, and AH and DL alpha diversity values were similar. It may be difficult to capture a general microbial alpha diversity response to SCTLD across coral species, as alpha diversity values are highly species-specific [28]. However, there were differences in microbial composition between AH and DL. In DL, the microbial community transitioned into an enrichment of Rhodobacterales and Peptostreptococcales-Tissierellales, which belong to the classes Alphaproteobacteria and Clostridia, respectively. Clostridia are anaerobic [46] and while Rhodobacterales are generally aerobic [47] they can thrive in anoxic conditions [48]. This suggests that as the disease state transitions from DU to DL, the lesion may progress to anoxic conditions, as seen in black band disease [49]. However, presently it cannot be determined if that is a result of actions by the bacteria or if their enrichment is based on the shifting lesion environment [50]. Nonetheless, these two classes showed the highest connectivity and presence in the network analysis.

Across SCTLD microbiome studies, Rhodobacterales has been reported as highly abundant in all except one [26], and while Peptostreptococcales-Tissierellales has been

found enriched in some studies [15, 16, 27, 28], Clostridia has been significantly enriched in all of them [11, 15, 16, 23, 26–28]. Rhodobacterales may be more generally associated with coral diseases, as many of the taxa associated with SCTLD were also found in the *Acropora* spp. RTL study. In contrast, Peptostreptococcales-Tissierellales was not found in RTL and a BLAST search of these ASVs showed that only one had 100% similarity to a sequence in the database, from a study that examined soil polluted by crude oil [49]. The rest were less than 94.31% similar to the NCBI 16S rRNA database, suggesting these taxa may be unique to SCTLD. Analysis of inferred functional traits showed that Clostridia taxa may have important roles in lesion progression through pathways such as phospholipase C / alpha-toxin, a toxin found in Clostridia such as *Clostridium perfringens* [52] and a top pathway predicted in DL in this study. Phospholipase C / alpha-toxin is a metalloenzyme, dependent on zinc ions, which through lipid signaling degrades eukaryotic cell membranes, potentially resulting in necrosis [52]. Thus, Peptostreptococcales-Tissierellales could be contributing to tissue loss in SCTLD via an alpha-toxin. Overall, the high network connectivity and inferred functional potential of toxin production suggest that Clostridia may have a particularly important role in SCTLD bacterial interactions and lesion progression. Therefore, promising future directions for SCTLD microbiome research could include developing enrichment media for Clostridia [53] and then conducting knockout gene studies of the alpha toxin genes [54].

Future SCTLD studies may consider sampling less-studied coral species

In this meta-analysis, only half of the coral species impacted by this disease were evaluated [2]. While we found consistent bacterial enrichment between analyses with and without the two most frequently sampled coral species, coral species was found to be the main factor driving microbial community structure. Therefore, analyzing representatives of all susceptible coral species could be especially important in further narrowing down the microbial taxa specific to SCTLD. Future studies could consider including coral species with no or low sampling representation in their permits to enable opportunistic sampling, which when pooled together in a collaborative analysis such as this, may yield meaningful results.

Conclusions

This is the largest microbiome meta-analysis ever conducted on a single coral disease. We found differences in the microbiomes of apparently healthy (AH) corals between SCTLD zones (vulnerable, endemic, and epidemic). In endemic and epidemic zones, AH corals may have acquired SCTLD-associated bacteria, potentially representing a compromised health state or resistance. We also identified that dominant taxa varied depending on whether the samples were collected away from the lesion (DU) or near the lesion (DL) on a colony with SCTLD. In DU samples, Flavobacteriales and Synechococcales were the dominant taxa, but in DL Rhodobacterales and Peptostreptococcales-Tissierellales were dominant and were key taxa in structuring microbial networks. This indicates that there is a shift of dominant bacterial taxa during disease progression and implies the lesion tissue may become anoxic. Specifically,

513 during lesion progression, Peptostreptococcales-Tissierellales may be involved in tissue
514 loss by lysing coral and symbiont cells through the phospholipase C / alpha-toxin
515 pathway. Peptostreptococcales-Tissierellales taxa also appear to be more specifically
516 associated with SCTLD and not coral disease generalists, as some of the ASVs found
517 here have not been reported in other coral diseases.
518
519 Our findings convey the need for further focus on the transition of bacterial taxa from
520 DU to DL and characterization of the role of Peptostreptococcales-Tissierellales in
521 lesion progression. A key aspect of this future work could be the inclusion of a wider
522 assortment of coral species and compartments to better clarify the mechanisms of
523 SCTLD. In addition, more holistic studies are needed to understand SCTLD. The
524 bacterial community appears to play a role in SCTLD, but other members of the
525 holobiont (i.e., viruses and Symbiodiniaceae) may be contributing to this change.
526 Combining multiple methods such as culturing, metagenomics, metatranscriptomics,
527 and microscopy could help better clarify the microbial disease dynamics in SCTLD.
528

529 # Methods

530 ## Obtaining studies

531

532 To acquire small subunit (SSU) 16S rRNA datasets for this meta-analysis, an email was
533 sent on July 14, 2020, and July 23, 2020, to the hosts of the coral-list listserv and the
534 SCTLD Disease Advisory Committee (DAC) email list, requesting scientists to share
535 unpublished SCTLD-associated microbiome datasets. To allow for comparisons of

536 microbiomes between a past Caribbean coral disease to the novel SCTLD outbreak, a
537 rapid tissue loss (RTL) disease study in *Acropora palmata* (APAL) and *Acropora*
538 *cervicornis* (ACER) comprising apparently healthy (AH) samples, inoculated AH
539 samples, and inoculated diseased samples [55], also was included in some analyses.
540 This particular study was selected because *Acropora* spp. reportedly are not susceptible
541 to SCTLD and the study used V4 primers [3]. In total 17 studies were analyzed, 16 from
542 SCTLD and one from an *Acropora* spp. RTL study (Supplemental Table 1).
543
544 Study authors were requested to complete a pre-formatted metadata file to facilitate
545 comparisons of data across studies. Requested metadata included sample handling
546 information (e.g. source laboratory, sample collector) and ecological information (e.g.
547 source reef name, coordinates, zone, water temperature, and coral colony
548 measurements). SCTLD zones included vulnerable (where the disease had not yet
549 arrived), endemic (where the initial outbreak of the disease had moved through and no
550 or few active lesions were observed on colonies), and epidemic (where the outbreak
551 was active and prevalent across colonies of multiple species). Invasion zone sites,
552 where the disease was newly-arrived but not yet prevalent, were grouped within the
553 epidemic zone for consistency across studies and simplicity of analysis. Some metadata
554 required standardization of units and not all metadata were available across all studies.
555 However, in all field-collected samples, all sampling dates and reef site information were
556 available, enabling the completion of SCTLD disease zone metadata for Florida studies
557 by referencing the Coral Reef Evaluation and Monitoring Project, Disturbance Response
558 Monitoring, and SCTLD boundary reconnaissance databases. For USVI, zones were

559 assigned based on the USVI Department of Planning and Natural Resources SCTLD
560 database (https://dpnr.vi.gov/czm/sctld/).
561
562 **Bioinformatics to process sequence data**
563
564 Each sequencing run was imported to QIIME2-2022.2 [56, 57] and processed
565 individually. The datasets were divided into two distinct pipelines: (1) data that targeted
566 the 16S rRNA gene V4 region of Bacteria and/or Archaea and (2) data that targeted the
567 V3-V4 region of Bacteria and/or Archaea. For V4 datasets, the data were processed
568 with cut-adapt to remove sequencing primers corresponding to the respective study
569 [58]. In total, three 515F primers that targeted the V4 region of the 16S rRNA gene were
570 used across studies ('5-GTGCCAGCMGCCGCGGTAA-3' [n=1,033] [33], '5-
571 GTGYCAGCMGCCGCGGTAA-3' [n=1,219] [35], and '5-
572 ACACTGACGACATGGTTCTACAGTGCCAGCMGCCGCGGTAA-3', [n=79] [33, 34];
573 Supplemental Table 1). Next, the data were processed with DADA2 for quality control
574 and denoising using a max error rate of three [59]. Although all runs were paired-end
575 reads, the V4 samples were processed as single-end reads and the forward reads were
576 truncated at 130 base pairs (bp) with the DADA2 program. The error rates, truncation,
577 and single-end options were selected based on the quality and sequence length
578 (Supplemental Table 1) of the lowest quality reads across all datasets. The two V3-V4
579 datasets (n=31 samples) were processed with the cut-adapt program, which was used
580 to select forward sequences that contained sequences similar to the 515F primers used
581 in the V4 studies. The forward primer 515FY [35] was used as the target sequence

582 using a 0.4 error rate to allow for some differences in bases. The selected sequences
583 were then processed with DADA2 and truncated at 240 bps with a max error rate of
584 one. After, if studies had multiple Illumina sequencer runs, they were first merged
585 together, and then all studies were merged into one count table and sequence file. The
586 vsearch cluster-features-de-novo function was then used to cluster the data by 99%
587 similarity [60]. The classify-consensus-vsearch option was then used for taxonomy
588 assignments with the SILVA-138-99 database [61]. The data were then filtered to
589 remove mitochondria and chloroplast reads.
590

591 **Alpha diversity**

592

593 Shannon diversity metrics were generated with the phyloseq function
594 rarefy_even_depth with option replace=TRUE, and a minimum sequence depth for a
595 sample of 1000. Prior to rarefaction, taxa with a sum of zero across the subsetted data
596 were removed. Two sets of alpha diversity analyses were run: (1) evaluated differences
597 across the three zones (vulnerable, endemic, and epidemic) in field-sourcws apparently
598 healthy (AH) corals, and (2) evaluated differences across disease states (AH,
599 unaffected tissue [DU], and lesion tissue [DL] on a diseased colony) in SCTLD-
600 susceptible corals (i.e., without *Acropora* spp.). Significance was tested with linear
601 mixed models with the R packages lme4 v1.1.21 [62], and emmeans v1.4.3.1 [63], and
602 for pairwise comparisons Tukey's HSD was used. For zones and disease states, coral
603 species was used as a random effect.
604

Beta diversity

The data were imported into R v4.0.5 and converted into a phyloseq object [64]. ASVs were removed if they were present less than four times in 20% of the samples. The filtered count table was transformed using centered log-ratio (CLR) with the package microbiome [65]. Beta diversity was analyzed with the package VEGAN 2.5.4 [66] and the filtered CLR-transformed table. The function vegdist was used to generate dissimilarity indices with a Euclidean distance. To identify significant differences among groups, a Permutational Multivariate Analysis of Variance (PERMANOVA) was used with the function adonis2 with 999 permutations, using a Euclidean distance. The function betadisper was used to calculate group dispersion, which was then tested for significance with the function Permutest.

Differences in beta diversity for field samples were evaluated in apparently healthy (AH) corals across three zones (vulnerable, endemic, and epidemic), and blocked by location (Florida vs USVI). In addition, pairwise group comparison was assessed from betadisper output using the Tukey's HSD function. The PERMANOVA output was also tested for pairwise comparisons with the function pairwise.adonis and adjusted with a Bonferroni correction [67]. Furthermore, all samples (including *Acropora* spp., sediment, and seawater) were also evaluated for beta diversity differences in primers, year of collection, biome (field and aquaria), studies, coral species, and sample type (seawater, mucus, tissue slurry, tissue slurry and skeleton, and sediment). These factors were also correlated to principal components (PCs) using the R package PCAtools 2.5.15, and the

functions pca and eigencorplot were used to remove the lowest 10% of the variance and to correlate the data and test for significance, respectively.

SCTLD-susceptible coral samples (i.e., without *Acropora* spp., sediment, and seawater) were also evaluated for beta-diversity. Both biomes (aquaria or field) were examined together and also separately. The matrices were generated with QIIME2-2021.11 with the plugin DEICODE, which runs a robust Aitchison Distance – a method that is not influenced by zeros in the data [68]. This was then evaluated for dispersion, differences in microbial composition between groups, and pairwise comparisons. DEICODE was also applied to the data without the two most prevalent corals species, *Orbicella faveolata* (OFAV) and *Montastraea cavernosa* (MCAV), to see if the same pattern was evident in disease states with and without these coral species.

Differential abundance analysis

The program Analysis of Compositions of Microbiomes with Bias Correction (ANCOM_BC) was used to identify differentially abundant microbial taxa [69]. ANCOM_BC was used with the global test option and the results were considered significant if the false discovery rate adjusted p-value (padj) was <0.001 and if the W statistic was >90. Field-sourced AH samples were tested for differential abundance among zones (vulnerable, endemic, and epidemic), and SCTLD-susceptible coral samples (without *Acropora* spp.) were evaluated for differences in disease state (AH, DU, and DL). For SCTLD-susceptible corals, the data were parsed by the three coral

651 compartments (mucus, tissue slurry, and tissue slurry skeleton). Sistinct ANCOM_BC
652 analyses were run for each compartment due to the relatively low sample size of tissue
653 slurry skeleton samples compared to the two other compartment types. The taxa were
654 further evaluated if they had a log-fold change between -1.5< and >1.5. The ASVs that
655 were significantly enriched were used to identify the relative abundance of the ASVs
656 across sample types. In addition, those enriched only in either DU or DL were used to
657 identify the presence or absence of each ASV in coral species and study per biome.
658 The same ANCOM_BC analysis was repeated without MCAV and OFAV to evaluate if
659 the two dominant coral species in our meta-analysis were driving the enriched bacteria.

660 **Network analysis**

661 To identify ASVs that co-associate in AH, DU, and DL samples, CLR-transformed
662 counts were used for weighted correlation network analysis (WGCNA) with the WGCNA
663 1.70-3 R package [70]. The network was constructed unsigned with the following
664 parameters: power=3, minimum module size=12, deep split=2, and merged cut
665 height=0.25. The eigenvalues were correlated to AH, DU, and DL using Pearson
666 correlation with the R function cor. The highest correlation in each disease state was
667 then selected for network construction using the R package SpiecEasi 1.0.5 [71]. The
668 network was then constructed as previously reported [11]. Briefly, the Stability Approach
669 to Regularization Selection (StARS) [72] model was chosen along with the method
670 Meinshausen-Bühlmann's neighborhood selection [73]. For StARS, 100 subsamples
671 were used with a variability threshold of 10^{-3}. The centrality (node importance) was
672 evaluated [74] using the functions centrality_degree (neighbors=the number of adjacent

673 edges or neighbors) and centrality_edge_betweenness (centrality=the number of
674 shortest paths going through an edge) [75]. The package influenceR 0.1.0. [76] selected
675 important ASVs in each network and assigned the top “key players” [77], which were
676 labeled with their respective orders.
677

678 **Functional prediction profiles**

679 To infer the functional potential of 16S rRNA gene data among AH, DU, and DL, the
680 program Phylogenetic Investigation of Communities by Reconstruction of Unobserved
681 States (PICRUSt2) was used in QIIME2-2021.11 [78]. Only SCTLD-susceptible corals
682 were evaluated and only ASVs that were present in at least 100 samples were selected.
683 The picrust2 full-pipeline was used with the hidden state set to “mp” and the placement
684 tool to place sequences into a tree set to “epa-ng.” The outputs were predicted
685 metagenomes for Kyoto Encyclopedia of Genes and Genomes (KEGG [79]) orthologs
686 and MetaCyc pathway [80] abundances. To assess the differential abundance of these
687 outputs among disease states, the R package Maaslin2 was utilized [81]. For both
688 KEGG and MetaCyc tests, data were log-transformed, a random effect was set to coral
689 species, and the data were subsequently analyzed with a linear model. In the KEGG
690 assessment, the minimum abundance=0.05 and the minimum prevalence=0.1. There
691 were no minimums set for the MetaCyc test due to the lower number of pathways found
692 in MetaCyc. The top 10 predicted pathways were selected based on values with the
693 lowest padj and effect sizes <-0.5 and >0.5. These pathways were manually annotated
694 on KEGG and MetaCyc websites.
695

696

697 Acknowledgments

698 Any use of trade, firm, or product names is for descriptive purposes only and does not
699 imply endorsement by the U.S. Government. We would like to thank the Disease
700 Advisory Committee Pathogen ID/Microbiome sub-team which spawned the “Sweet
701 16S” team that led to this paper. SMR was supported by National Oceanic and
702 Atmospheric Administration (NOAA) Office of Oceanic and Atmospheric Research
703 (OAR) omics initiative. LKH was supported by Environmental Protection Agency South
704 Florida Initiative grants X7-00D66417-0 and X7-01D00820-0. JSE, CAK, and WBS were
705 supported by the USGS Ecosystems Biological Threats & Invasive Species Research
706 Program. AA was supported by National Science Foundation awards 1938112 and
707 2109622 and a NOAA OAR Cooperative Institutes award. EMM was supported by a
708 Mote Eminent Scholarship. ENS and JDV were supported by Florida Department of
709 Environmental Protection, Professional Association of Diving Instructors, and the Harbor
710 Branch Oceanographic Institute Foundation.

711

712 Conflict of interest

713 The authors declare that they have no conflict of interest.

714

715 Data availability statement

716 Sequence data available on NCBI are listed in Supplemental Table 1. All other datasets
717 are available upon request. The unfiltered ASV counts table, taxonomy table, ASV

718 sequences, and code to conduct this analysis are publicly available at
719 https://github.com/srosales712/SCTLD_microbiome_meta_analysis.
720

721 # References

722 1. Landsberg JH, Kiryu Y, Peters EC, Wilson PW, Perry N, Waters Y, et al. Stony Coral
723 Tissue Loss Disease in Florida is Associated with Disruption of Host–Zooxanthellae
724 Physiology. *Front Mar Sci* 2020; **7**: 576013.
725 2. Case Definition: Stony Coral Tissue Loss Disease (SCTLD). Available online
726 at: https://floridadep.gov/sites/default/files/Copy%20of%20StonyCoralTissueLossDi
727 sease_CaseDefinition%20final%2010022018.pdf (accessed July 14, 2022)
728 3. Precht WF, Gintert BE, Robbart ML, Fura R, van Woesik R. Unprecedented Disease-
729 Related Coral Mortality in Southeastern Florida. *Sci Rep* 2016; **6**.
730 4. Miller M, Karazsia J, Groves CE, Griffin S, Moore T, Wilber P, et al. Detecting
731 sedimentation impacts to coral reefs resulting from dredging the Port of Miami, Florida
732 USA. *PeerJ* 2016; **4**: e2711.
733 5. Walton CJ, Hayes NK, Gilliam DS. Impacts of a Regional, Multi-Year, Multi-Species Coral
734 Disease Outbreak in Southeast Florida. *Front Mar Sci* 2018; **5**.
735 6. Gintert BE, Precht WF, Fura R, Rogers K, Rice M, Precht LL, et al. Regional coral disease
736 outbreak overwhelms impacts from a local dredge project. *Environ Monit Assess* 2019;
737 **191**.
738 7. Alvarez-Filip L, Estrada-Saldívar N, Pérez-Cervantes E, Molina-Hernández A, González-
739 Barrios FJ. A rapid spread of the stony coral tissue loss disease outbreak in the Mexican
740 Caribbean. *PeerJ* 2019; **7**: e8069.
741 8. Alvarez-Filip L, González-Barrios FJ, Pérez-Cervantes E, Molina-Hernández A, Estrada-

742 Saldívar N. Stony coral tissue loss disease decimated Caribbean coral populations and
743 reshaped reef functionality. *Commun Biol* 2022; **5**: 440.
744 9. Williams SD, Walter CS, Muller EM. Fine Scale Temporal and Spatial Dynamics of the
745 Stony Coral Tissue Loss Disease Outbreak Within the Lower Florida Keys. *Front Mar Sci*
746 2021; **8**: 631776.
747 10. Hayes NK, Walton CJ, Gilliam DS. Tissue loss disease outbreak significantly alters the
748 Southeast Florida stony coral assemblage. *Front Mar Sci* 2022; **9**: 975894.
749 11. Rosales SM, Clark AS, Huebner LK, Ruzicka RR, Muller EM. Rhodobacterales and
750 Rhizobiales are Associated with Stony Coral Tissue Loss Disease and its Suspected
751 Sources of Transmission. *Front Microbiol* 2020; **11**.
752 12. Studivan MS, Rossin AM, Rubin E, Soderberg N, Holstein DM, Enochs IC. Reef Sediments
753 can act as a Stony Coral Tissue Loss Disease vector. *Front Mar Sci* 2022; **8**: 815698.
754 13. Work TM, Weatherby TM, Landsberg JH, Kiryu Y, Cook SM, Peters EC. Viral-like particles
755 are associated with endosymbiont pathology in Florida corals affected by Stony Coral
756 Tissue Loss Disease. *Front Mar Sci* 2021; **8**: 750658.
757 14. Veglia AJ, Beavers K, Van Buren EW, Meiling SS, Muller EM, Smith TB, et al.
758 Alphaflexivirus Genomes in Stony Coral Tissue Loss Disease-Affected, Disease-Exposed,
759 and Disease-Unexposed Coral Colonies in the U.S. Virgin Islands. *Microbiol Resour*
760 *Announc* 2022; **11**: e01199-21.
761 15. Meyer JL, Castellanos-Gell J, Aeby GS, Häse CC, Ushijima B, Paul VJ. Microbial
762 Community Shifts Associated With the Ongoing Stony Coral Tissue Loss Disease
763 Outbreak on the Florida Reef Tract. *Front Microbiol* 2019; **10**: 2244.
764 16. Huntley N, Brandt ME, Becker CC, Miller CA, Meiling SS, Correa AMS, et al. Experimental
765 transmission of Stony Coral Tissue Loss Disease results in differential microbial responses
766 within coral mucus and tissue. *ISME Commun* 2022; **2**: 46.
767 17. Muller EM, Sartor C, Alcaraz NI, van Woesik R. Spatial Epidemiology of the Stony-Coral-

Tissue-Loss Disease in Florida. *Front Mar Sci* 2020; **7**: 163.

18. Meiling S, Muller EM, Smith TB, Brandt ME. 3D Photogrammetry Reveals Dynamics of Stony Coral Tissue Loss Disease (SCTLD) Lesion Progression Across a Thermal Stress Event. *Front Mar Sci* 2020; **7**: 597643.

19. Aeby GS, Ushijima B, Campbell JE, Jones S, Williams GJ, Meyer JL, et al. Pathogenesis of a Tissue Loss Disease Affecting Multiple Species of Corals Along the Florida Reef Tract. *Front Mar Sci* 2019; **6**.

20. Dobbelaere T, Muller EM, Gramer LJ, Holstein DM, Hanert E. Coupled Epidemio-Hydrodynamic Modeling to Understand the Spread of a Deadly Coral Disease in Florida. *Front Mar Sci* 2020; **7**: 591881.

21. Eaton KR, Landsberg JH, Kiryu Y, Peters EC, Muller EM. Measuring Stony Coral Tissue Loss Disease Induction and Lesion Progression Within Two Intermediately Susceptible Species, *Montastraea cavernosa* and *Orbicella faveolata*. *Front Mar Sci* 2021; **8**: 717265.

22. Aeby GS, Ushijima B, Campbell JE, Jones S, Williams GJ, Meyer JL, et al. Pathogenesis of a Tissue Loss Disease Affecting Multiple Species of Corals Along the Florida Reef Tract. *Front Mar Sci* 2019; **6**: 678.

23. Rosales SM, Huebner LK, Clark AS, McMinds R, Ruzicka RR, Muller EM. Bacterial Metabolic Potential and Micro-Eukaryotes Enriched in Stony Coral Tissue Loss Disease Lesions. *Front Mar Sci* 2022; **8**: 776859.

24. Landsberg JH, Kiryu Y, Peters EC, Wilson PW, Perry N, Waters Y, et al. Stony Coral Tissue Loss Disease in Florida Is Associated With Disruption of Host–Zooxanthellae Physiology. *Front Mar Sci* 2020; **7**: 576013.

25. Iwanowicz DD, Schill WB, Woodley CM, Bruckner A, Neely K, Briggs KM. Exploring the Stony Coral Tissue Loss Disease Bacterial Pathobiome. 2020. Microbiology.

26. Thome PE, Rivera-Ortega J, Rodríguez-Villalobos JC, Cerqueda-García D, Guzmán-Urieta EO, García-Maldonado JQ, et al. Local dynamics of a white syndrome outbreak and

794 changes in the microbial community associated with colonies of the scleractinian brain
795 coral *Pseudodiploria strigosa*. *PeerJ* 2021; **9**: e10695.
796 27. Becker CC, Brandt M, Miller CA, Apprill A. Microbial bioindicators of Stony Coral Tissue
797 Loss Disease identified in corals and overlying waters using a rapid field-based
798 sequencing approach. *Environ Microbiol* 2021; 1462-2920.15718.
799 28. Clark AS, Williams SD, Maxwell K, Rosales SM, Huebner LK, Landsberg JH, et al.
800 Characterization of the Microbiome of Corals with Stony Coral Tissue Loss Disease along
801 Florida's Coral Reef. *Microorganisms* 2021; **9**: 2181.
802 29. Evans JS, Paul VJ, Ushijima B, Kellogg CA. Combining tangential flow filtration and size
803 fractionation of mesocosm water as a method for the investigation of waterborne coral
804 diseases. *Biol Methods Protoc* 2022; **7**: bpac007.
805 30. Neely KL, Macaulay KA, Hower EK, Dobler MA. Effectiveness of topical antibiotics in
806 treating corals affected by Stony Coral Tissue Loss Disease. *PeerJ* 2020; **8**: e9289.
807 31. Walker BK, Turner NR, Noren HKG, Buckley SF, Pitts KA. Optimizing Stony Coral Tissue
808 Loss Disease (SCTLD) Intervention Treatments on *Montastraea cavernosa* in an Endemic
809 Zone. *Front Mar Sci* 2021; **8**: 666224.
810 32. The Microbiome Quality Control Project Consortium, Sinha R, Abu-Ali G, Vogtmann E,
811 Fodor AA, Ren B, et al. Assessment of variation in microbial community amplicon
812 sequencing by the Microbiome Quality Control (MBQC) project consortium. *Nat Biotechnol*
813 2017; **35**: 1077–1086.
814 33. Caporaso JG, Lauber CL, Walters WA, Berg-Lyons D, Lozupone CA, Turnbaugh PJ, et al.
815 Global patterns of 16S rRNA diversity at a depth of millions of sequences per sample. *Proc*
816 *Natl Acad Sci* 2011; **108**: 4516–4522.
817 34. Green SJ, Venkatramanan R, Naqib A. Deconstructing the Polymerase Chain Reaction:
818 Understanding and Correcting Bias Associated with Primer Degeneracies and Primer-
819 Template Mismatches. *PLOS ONE* 2015; **10**: e0128122.

820 35. Parada AE, Needham DM, Fuhrman JA. Every base matters: assessing small subunit
821 rRNA primers for marine microbiomes with mock communities, time series and global field
822 samples: Primers for marine microbiome studies. *Environ Microbiol* 2016; **18**: 1403–1414.
823 36. Apprill A, McNally S, Parsons R, Weber L. Minor revision to V4 region SSU rRNA 806R
824 gene primer greatly increases detection of SAR11 bacterioplankton. *Aquat Microb Ecol*
825 2015; **75**: 129–137.
826 37. Herlemann DP, Labrenz M, Jürgens K, Bertilsson S, Waniek JJ, Andersson AF.
827 Transitions in bacterial communities along the 2000 km salinity gradient of the Baltic Sea.
828 *ISME J* 2011; **5**: 1571–1579.
829 38. Takai K, Horikoshi K. Rapid Detection and Quantification of Members of the Archaeal
830 Community by Quantitative PCR Using Fluorogenic Probes. *Appl Environ Microbiol* 2000;
831 **66**: 5066–5072.
832 39. McDevitt-Irwin JM, Baum JK, Garren M, Vega Thurber RL. Responses of Coral-Associated
833 Bacterial Communities to Local and Global Stressors. *Front Mar Sci* 2017; **4**.
834 40. Galand PE, Chapron L, Meistertzheim A-L, Peru E, Lartaud F. The Effect of Captivity on
835 the Dynamics of Active Bacterial Communities Differs Between Two Deep-Sea Coral
836 Species. *Front Microbiol* 2018; **9**: 2565.
837 41. Dang H, Li T, Chen M, Huang G. Cross-Ocean Distribution of *Rhodobacterales* Bacteria as
838 Primary Surface Colonizers in Temperate Coastal Marine Waters. *Appl Environ Microbiol*
839 2008; **74**: 52–60.
840 42. Welsh RM, Rosales SM, Zaneveld JR, Payet JP, McMinds R, Hubbs SL, et al. Alien vs.
841 predator: bacterial challenge alters coral microbiomes unless controlled by
842 *Halobacteriovorax* predators. *PeerJ* 2017; **5**: e3315.
843 43. Shilling EN, Combs IR, Voss JD. Assessing the effectiveness of two intervention methods
844 for stony coral tissue loss disease on *Montastraea cavernosa*. *Sci Rep* 2021; **11**: 8566.
845 44. Hadaidi G, Ziegler M, Shore-Maggio A, Jensen T, Aeby G, Voolstra CR. Ecological and

molecular characterization of a coral black band disease outbreak in the Red Sea during a bleaching event. *PeerJ* 2018; **6**: e5169.

45. de Castro AP, Araújo SD, Reis AMM, Moura RL, Francini-Filho RB, Pappas G, et al. Bacterial Community Associated with Healthy and Diseased Reef Coral *Mussismilia hispida* from Eastern Brazil. *Microb Ecol* 2010; **59**: 658–667.

46. Dürre P. Clostridia. In: John Wiley & Sons, Ltd (ed). *eLS*, 1st ed. 2015. Wiley, pp 1–11.

47. Pujalte MJ, Lucena T, Ruvira MA, Arahal DR, Macián MC. The Family Rhodobacteraceae. In: Rosenberg E, DeLong EF, Lory S, Stackebrandt E, Thompson F (eds). *The Prokaryotes*. 2014. Springer Berlin Heidelberg, Berlin, Heidelberg, pp 439–512.

48. Pohlner M, Dlugosch L, Wemheuer B, Mills H, Engelen B, Reese BK. The Majority of Active Rhodobacteraceae in Marine Sediments Belong to Uncultured Genera: A Molecular Approach to Link Their Distribution to Environmental Conditions. *Front Microbiol* 2019; **10**: 659.

49. Carlton RG, Richardson LL. Oxygen and sulfide dynamics in a horizontally migrating cyanobacterial mat: Black band disease of corals. *FEMS Microbiol Ecol* 1995; **18**: 155–162.

50. Hughes DJ, Raina J-B, Nielsen DA, Suggett DJ, Kühl M. Disentangling compartment functions in sessile marine invertebrates. *Trends Ecol Evol* 2022; S016953472200091X.

51. Tan H-Q, Wu X-Y, Zhang X-Q, Wu M, Zhu X-F. *Tepidibacter mesophilus* sp. nov., a mesophilic fermentative anaerobe isolated from soil polluted by crude oil, and emended description of the genus *Tepidibacter*. *Int J Syst Evol Microbiol* 2012; **62**: 66–70.

52. Urbina P, Collado MI, Alonso A, Goñi FM, Flores-Díaz M, Alape-Girón A, et al. Unexpected wide substrate specificity of *C. perfringens* α-toxin phospholipase C. *Biochim Biophys Acta BBA - Biomembr* 2011; **1808**: 2618–2627.

53. Anwar Z, Regan SB, Linden J. Enrichment and Detection of *Clostridium perfringens* Toxinotypes in Retail Food Samples. *J Vis Exp* 2019; 59931.

872 54. Chen Y, McClane BA, Fisher DJ, Rood JI, Gupta P. Construction of an Alpha Toxin Gene
873 Knockout Mutant of *Clostridium perfringens* Type A by Use of a Mobile Group II Intron.
874 *Appl Environ Microbiol* 2005; **71**: 7542–7547.
875 55. Rosales SM, Miller MW, Williams DE, Traylor-Knowles N, Young B, Serrano XM.
876 Microbiome differences in disease-resistant vs. susceptible *Acropora* corals subjected to
877 disease challenge assays. *Sci Rep* 2019; **9**.
878 56. Bolyen E, Rideout JR, Dillon MR, Bokulich NA, Abnet CC, Al-Ghalith GA, et al.
879 Reproducible, interactive, scalable and extensible microbiome data science using QIIME 2.
880 *Nat Biotechnol* 2019; **37**: 852–857.
881 57. Estaki M, Jiang L, Bokulich NA, McDonald D, González A, Kosciolek T, et al. QIIME 2
882 Enables Comprehensive End-to-End Analysis of Diverse Microbiome Data and
883 Comparative Studies with Publicly Available Data. *Curr Protoc Bioinforma* 2020; **70**.
884 58. Martin M. Cutadapt removes adapter sequences from high-throughput sequencing reads.
885 *EMBnet.journal* 2011; **17**: 10.
886 59. Callahan BJ, McMurdie PJ, Rosen MJ, Han AW, Johnson AJA, Holmes SP. DADA2: High-
887 resolution sample inference from Illumina amplicon data. *Nat Methods* 2016; **13**: 581–583.
888 60. Rognes T, Flouri T, Nichols B, Quince C, Mahé F. VSEARCH: a versatile open source tool
889 for metagenomics. *PeerJ* 2016; **4**: e2584.
890 61. Quast C, Pruesse E, Yilmaz P, Gerken J, Schweer T, Yarza P, et al. The SILVA ribosomal
891 RNA gene database project: improved data processing and web-based tools. *Nucleic*
892 *Acids Res* 2012; **41**: D590–D596.
893 62. Bates D, Mächler M, Bolker B, Walker S. Fitting Linear Mixed-Effects Models Using **lme4**.
894 *J Stat Softw* 2015; **67**.
895 63. Searle SR, Speed FM, Milliken GA. Population Marginal Means in the Linear Model: An
896 Alternative to Least Squares Means. *Am Stat* 1980; **34**: 216–221.
897 64. McMurdie PJ, Holmes S. phyloseq: An R Package for Reproducible Interactive Analysis

and Graphics of Microbiome Census Data. *PLoS ONE* 2013; **8**: e61217.

65. Leo Lahti et al. Tools for microbiome analysis in R. Microbiome package version. 2017. Bioconductor.

66. Dixon P. VEGAN, a package of R functions for community ecology. *J Veg Sci* 2003; **14**: 927.

67. Martinez A. pairwiseAdonis: Pairwise multilevel comparison using adonis. 2019.

68. Martino C, Morton JT, Marotz CA, Thompson LR, Tripathi A, Knight R, et al. A Novel Sparse Compositional Technique Reveals Microbial Perturbations. *mSystems* 2019; **4**: e00016-19.

69. Lin H, Peddada SD. Analysis of compositions of microbiomes with bias correction. *Nat Commun* 2020; **11**: 3514.

70. Langfelder P, Horvath S. WGCNA: an R package for weighted correlation network analysis. *BMC Bioinformatics* 2008; **9**: 559.

71. Kurtz ZD, Müller CL, Miraldi ER, Littman DR, Blaser MJ, Bonneau RA. Sparse and Compositionally Robust Inference of Microbial Ecological Networks. *PLOS Comput Biol* 2015; **11**: e1004226.

72. Han L, Roeder K, Wasserman L. Stability Approach to Regularization Selection (StARS) for High Dimensional Graphical Models. 2010.

73. Meinshausen N, Bühlmann P. High-dimensional graphs and variable selection with the Lasso. *Ann Stat* 2006; **34**: 1436–1462.

74. Thomas Lin Pederse. A Tidy API for Graph Manipulation. 2019.

75. Brandes U. A faster algorithm for betweenness centrality*. *J Math Sociol* 2001; **25**: 163–177.

76. Simon J. influenceR: Software Tools to Quantify Structural Importance of Nodes in a Network. 2015.

77. Borgatti SP. Identifying sets of key players in a social network. *Comput Math Organ Theory*

2006; **12**: 21–34.

78. Douglas GM, Maffei VJ, Zaneveld JR, Yurgel SN, Brown JR, Taylor CM, et al. PICRUSt2 for prediction of metagenome functions. *Nat Biotechnol* 2020; **38**: 685–688.

79. Kanehisa M. KEGG: Kyoto Encyclopedia of Genes and Genomes. *Nucleic Acids Res* 2000; **28**: 27–30.

80. Caspi R, Billington R, Keseler IM, Kothari A, Krummenacker M, Midford PE, et al. The MetaCyc database of metabolic pathways and enzymes - a 2019 update. *Nucleic Acids Res* 2020; **48**: D445–D453.

81. Mallick H, Rahnavard A, McIver LJ, Ma S, Zhang Y, Nguyen LH, et al. Multivariable association discovery in population-scale meta-omics studies. *PLOS Comput Biol* 2021; **17**: e1009442.

Figure 1. **The number of aquaria and field samples for each coral species** across (A) SSU rRNA gene primer sets, (B) sample type, and (C) disease state. NAs in (A) and (B) represent sediment and seawater samples. Coral species codes represent the following: *Acropora cervicornis* (ACER), *Acropora palmata* (APAL), *Colpophyllia natans* (CNAT), *Diploria labyrinthiformis* (DLAB), *Dichocoenia stokesii* (DSTO), *Montastraea cavernosa* (MCAV), *Meandrina meandrites* (MMEA), *Orbicella annularis* (OANN), *Orbicella faveolata* (OFAV), *Orbicella franksi* (OFRA), *Porites astreoides* (PAST), *Pseudodiploria clivosa* (PCLI), *Pseudodiploria strigosa* (PSTR), *Stephanocoenia intersepta* (SINT), *Siderastrea siderea* (SSID).

Figure 2. **Comparisons among microbial communities of field-sourced apparently healthy (AH) coral colonies across SCTLD zones (vulnerable, endemic, and epidemic) in Florida and the U.S. Virgin Islands** in (A) beta diversity (centered log-ratio transformed and plotted with a Euclidean distance), and differential abundance analysis in (B) vulnerable vs endemic zones, and (C) vulnerable vs epidemic zones. ASVs are grouped by genus (represented by dashes) on the y-axis and then by order, and only ASVs with a padj<0.001, a W statistic >90, and a log-fold change <-2 and >2 were visualized. AH samples from the three coral compartments (mucus, tissue slurry, and tissue slurry skeleton) were included and *Acopora* spp. samples were excluded from the analysis.

Figure 3. **Microbial beta diversity of all coral species (SCTLD-susceptible corals and *Acropora* spp.) and sample types (coral, sediment, and seawater) show differences within and between microbial communities** in (A) SSU 16S rRNA gene primers, (B) year, (C) biome, (D) study, (E) coral species, and (F) sample type. All plots were centered log-ratio transformed and visualized with a Euclidean distance. The NAs in (E) represent sediment and seawater samples; coral species codes are defined in Figure 1 legend.

Figure 4. **Microbial differences in coral disease state among apparently healthy colonies (AH), and unaffected (DU) and lesion (DL) areas on diseased colonies** in beta diversity of (A) both aquaria and field samples ("Combined"), (B) aquaria, and (C) field samples only. Samples from *Acropora* spp. were excluded and the three coral compartments (mucus, tissue slurry, and tissue slurry skeleton) were included in this analysis.

Figure 5. **Microbial ASVs associated with unaffected areas on diseased colonies (DU)**. Differential abundances between (A) apparently healthy (AH) vs DU. The y-axis depicts ASVs grouped by genus and then by order. Only ASVs with a padj<0.001, W statistic >90, and a log-fold change <-1.5 and >1.5 were visualized. Coral compartments (i.e., mucus, tissue slurry, and tissue slurry skeleton) were included and *Acropora* spp. were excluded from this analysis. (B) The relative abundance of taxa enriched in AH and DU by sample type.

Figure 6. **Microbial ASVs associated with lesions on diseased colonies (DL).** Differential abundances between (A) apparently healthy (AH) vs DL. The y-axis depicts ASVs grouped by genus and then by order. Only ASVs with a padj<0.001, W statistic >90, and a log-fold change <-1.5 and >1.5 were visualized. Coral compartments (i.e., mucus, tissue slurry, and tissue slurry skeleton) were included and *Acropora* spp. were excluded from this analysis. (B) The relative abundance of taxa enriched in AH and DL by sample type.

Figure 7. **Co-occurrence networks of bacteria from weighted correlation network analysis (WGCNA) modules** (Supplemental Fig 7) **among apparently healthy colonies (AH), and unaffected areas (DU) and lesions (DL) on diseased colonies.** The nodes represent amplicon sequence variants (ASV), which are sized by the ASV's correlation value to its respective module. A triangle and label of the bacteria order denote that a node is a "key player." The width of the edges corresponds to centrality, with thicker edges representing higher centrality. Samples from the three coral compartments (i.e., mucus, tissue slurry, and tissue slurry skeleton) were included in the analysis, and *Acropora* spp. samples were excluded from this analysis.

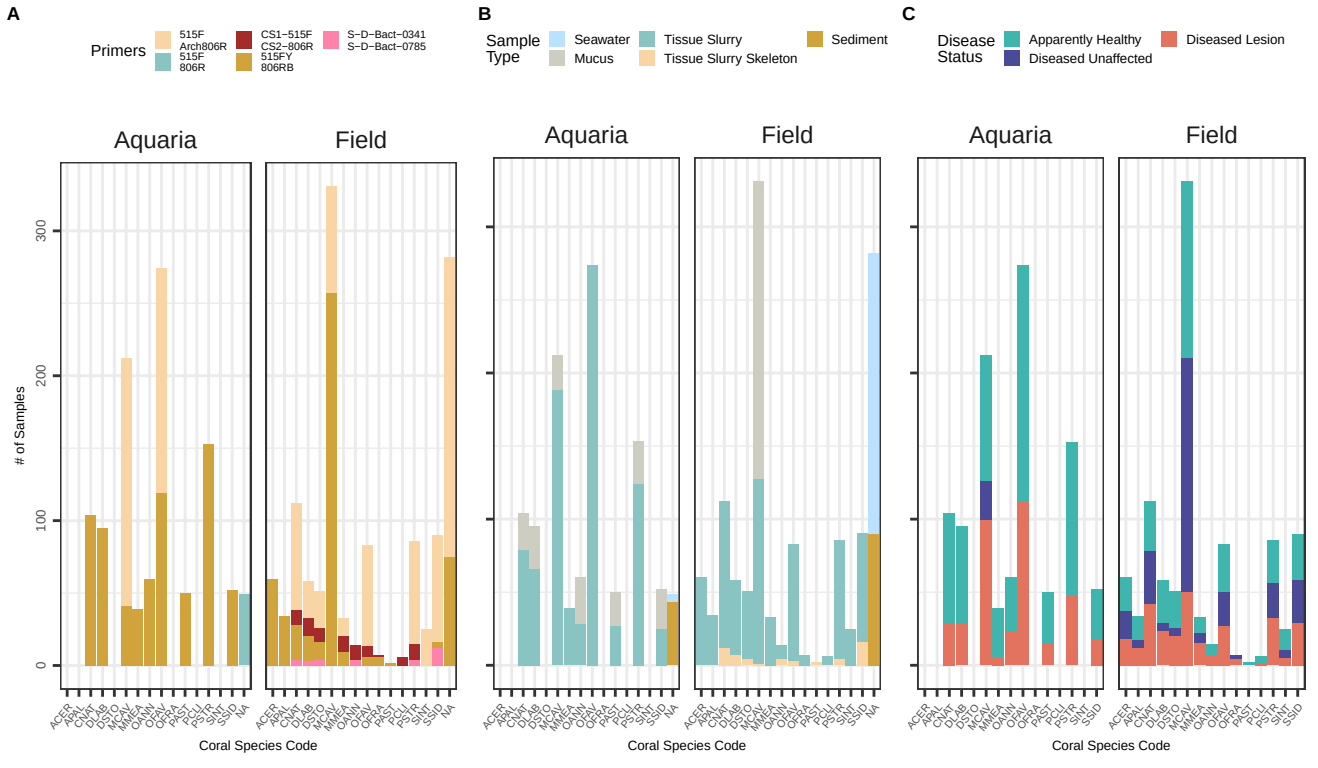
A
Primers
515F Arch806R
515F 806R
CS1−515F CS2−806R 515FY 806RB
S−D−Bact−0341 S−D−Bact−0785
B
Sample Type
Seawater
Mucus
Tissue Slurry
Tissue Slurry Skeleton
Sediment
C
Disease Status
Apparently Healthy
Diseased Unaffected
Diseased Lesion
Aquaria
Field
# of Samples
0
100
200
300
ACER APAL CNAT DLAB DSTO MCAV MMEA OANN OFAV OFAA PAST PCLI PSTR SINT SSID NA
Coral Species Code

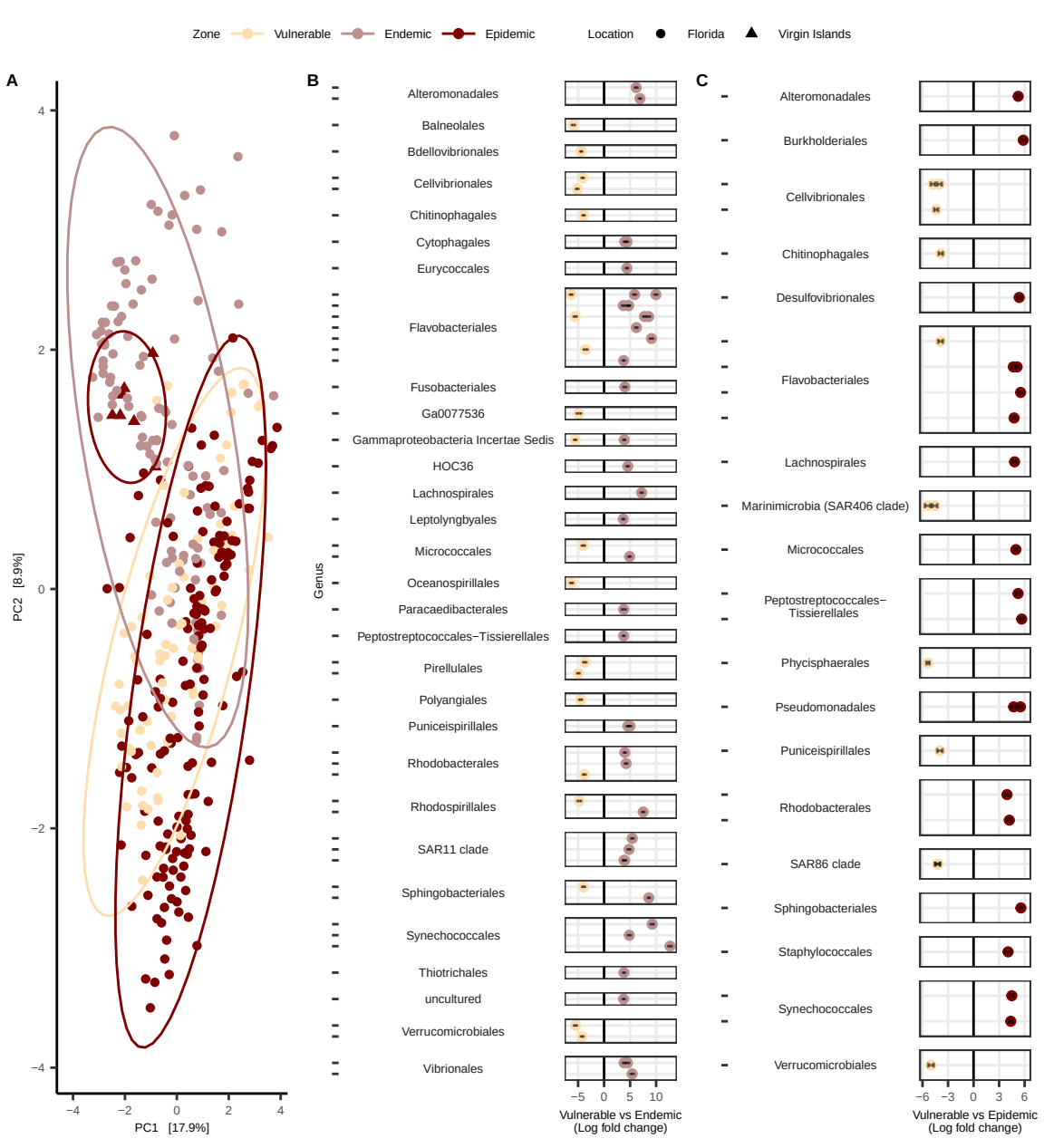
Zone
Vulnerable
Endemic
Epidemic
Location
Florida
Virgin Islands
A
B
C
PC1 [17.9%]
PC2 [8.9%]
Genus
Alteromonadales
Balneolales
Bdellovibrionales
Cellvibrionales
Chitinophagales
Cytophagales
Eurycoccales
Flavobacteriales
Fusobacteriales
Ga0077536
Gammaproteobacteria Incertae Sedis
HOC36
Lachnospirales
Leptolyngbyales
Micrococcales
Oceanospirillales
Paracaedibacterales
Peptostreptococcales−Tissierellales
Pirellulales
Polyangiales
Puniceispirillales
Rhodobacterales
Rhodospirillales
SAR11 clade
Sphingobacteriales
Synechococcales
Thiotrichales
uncultured
Verrucomicrobiales
Vibrionales
Vulnerable vs Endemic
(Log fold change)
Alteromonadales
Burkholderiales
Cellvibrionales
Chitinophagales
Desulfovibrionales
Flavobacteriales
Lachnospirales
Marinimicrobia (SAR406 clade)
Micrococcales
Peptostreptococcales−
Tissierellales
Phycisphaerales
Pseudomonadales
Puniceispirillales
Rhodobacterales
SAR86 clade
Sphingobacteriales
Staphylococcales
Synechococcales
Verrucomicrobiales
Vulnerable vs Epidemic
(Log fold change)

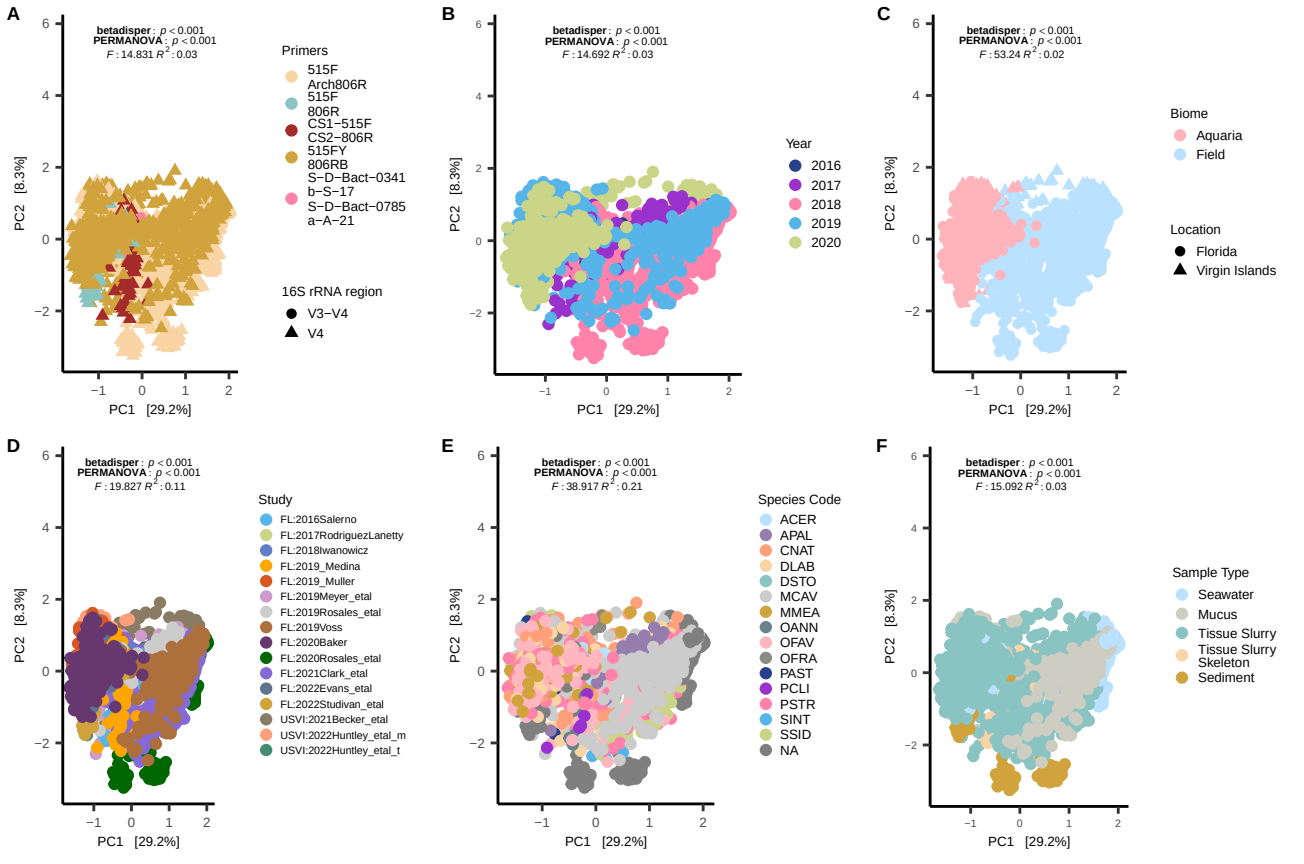
A
betadisper : p < 0.001
PERMANOVA : p < 0.001
F : 14.831 R2 : 0.03
Primers
515F
Arch806R
515F
806R
CS1−515F
CS2−806R
515FY
806RB
S−D−Bact−0341
b−S−17
S−D−Bact−0785
a−A−21
16S rRNA region
V3−V4
V4
PC2 [8.3%]
PC1 [29.2%]
B
betadisper : p < 0.001
PERMANOVA : p < 0.001
F : 14.692 R2 : 0.03
Year
2016
2017
2018
2019
2020
C
betadisper : p < 0.001
PERMANOVA : p < 0.001
F : 53.24 R2 : 0.02
Biome
Aquaria
Field
Location
Florida
Virgin Islands
D
betadisper : p < 0.001
PERMANOVA : p < 0.001
F : 19.827 R2 : 0.11
Study
FL:2016Salerno
FL:2017RodriguezLanetty
FL:2018Iwanowicz
FL:2019_Medina
FL:2019_Muller
FL:2019Meyer_etal
FL:2019Rosales_etal
FL:2019Voss
FL:2020Baker
FL:2020Rosales_etal
FL:2021Clark_etal
FL:2022Evans_etal
FL:2022Studivan_etal
USVI:2021Becker_etal
USVI:2022Huntley_etal_m
USVI:2022Huntley_etal_t
E
betadisper : p < 0.001
PERMANOVA : p < 0.001
F : 38.917 R2 : 0.21
Species Code
ACER
APAL
CNAT
DLAB
DSTO
MCAV
MMEA
OANN
OFAV
OFRA
PAST
PCLI
PSTR
SINT
SSID
NA
F
betadisper : p < 0.001
PERMANOVA : p < 0.001
F : 15.092 R2 : 0.03
Sample Type
Seawater
Mucus
Tissue Slurry
Tissue Slurry Skeleton
Sediment

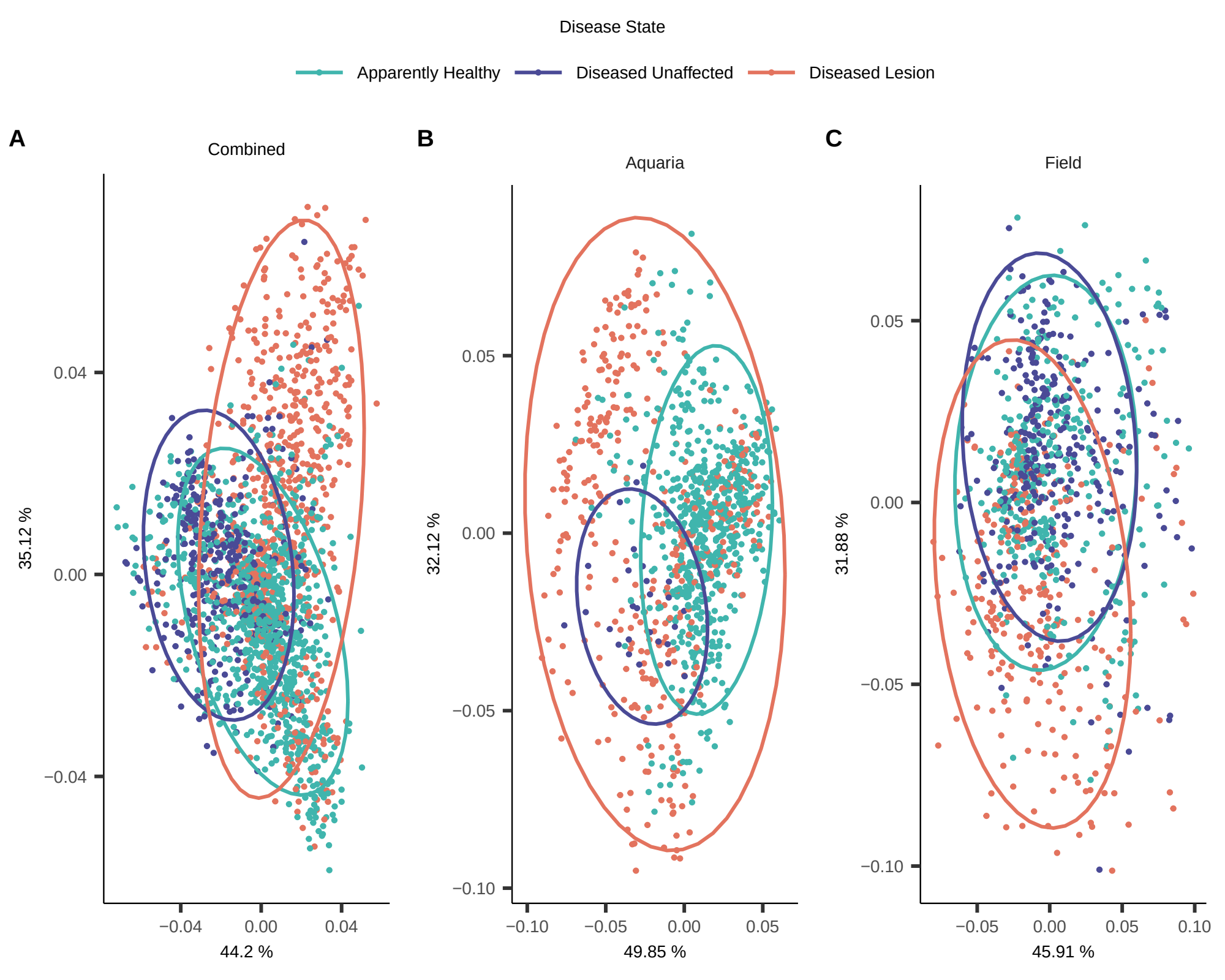
Disease State
Apparently Healthy
Diseased Unaffected
Diseased Lesion
A
Combined
B
Aquaria
C
Field
35.12 %
32.12 %
31.88 %
44.2 %
49.85 %
45.91 %
0.04
0.00
−0.04
0.05
−0.05
−0.10
0.10

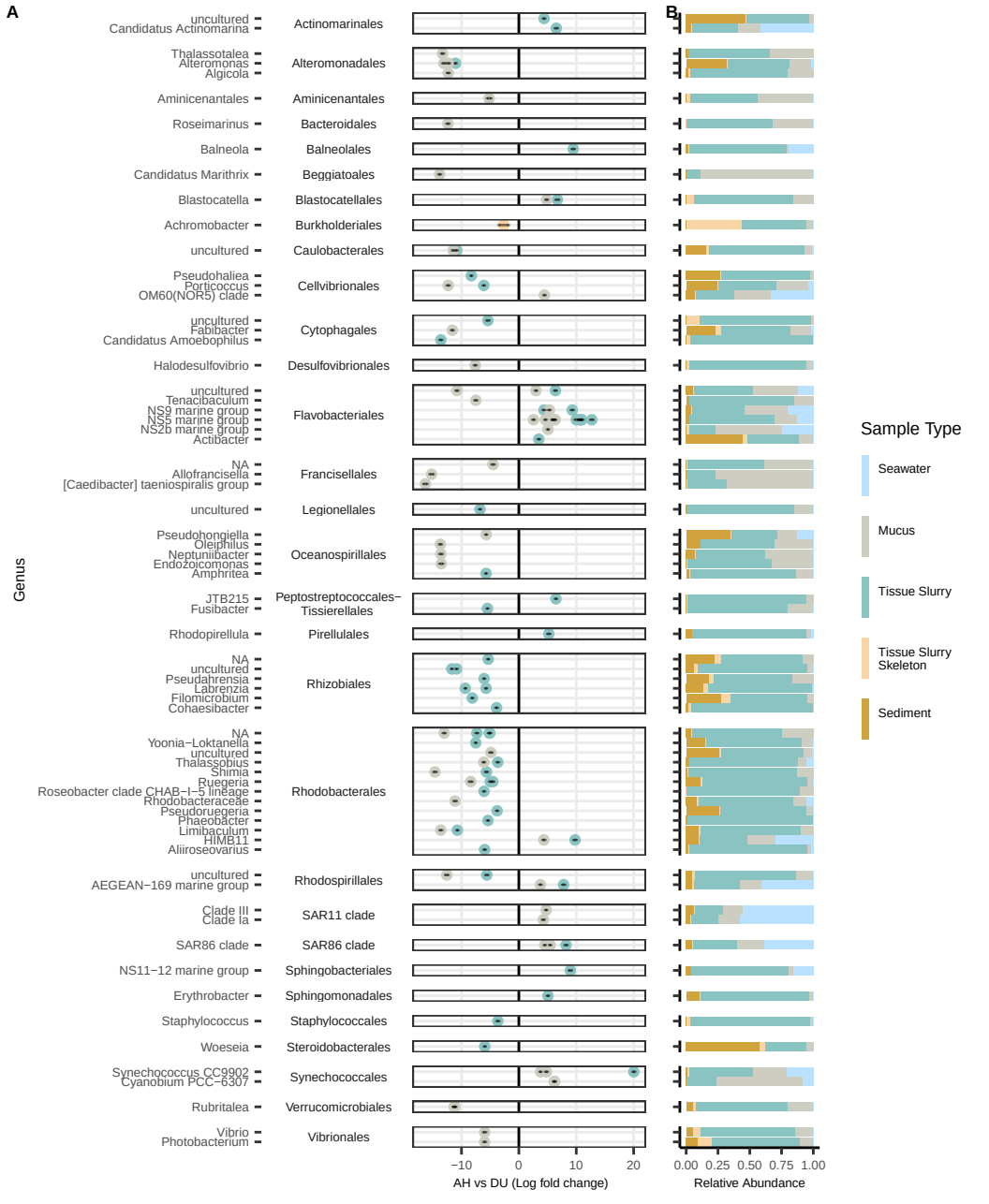
A
B
Genus
uncultured
Candidatus Actinomarina
Actinomarinales
Thalassotalea
Alteromonas
Algicola
Alteromonadales
Aminicenantales
Aminicenantales
Roseimarinus
Bacteroidales
Balneola
Balneolales
Candidatus Marithrix
Beggiatoales
Blastocatella
Blastocatellales
Achromobacter
Burkholderiales
uncultured
Caulobacterales
Pseudohaliea
Porticoccus
OM60(NOR5) clade
Cellvibrionales
uncultured
Fabibacter
Candidatus Amoebophilus
Cytophagales
Halodesulfovibrio
Desulfovibrionales
uncultured
Tenacibaculum
NS9 marine group
NS5 marine group
NS2b marine group
Actibacter
Flavobacteriales
NA
Allofrancisella
[Caedibacter] taeniospiralis group
Francisellales
uncultured
Legionellales
Pseudohongiella
Oleiphilus
Neptuniibacter
Endozoicomonas
Amphritea
Oceanospirillales
JTB215
Fusibacter
Peptostreptococcales−
Tissierellales
Rhodopirellula
Pirellulales
NA
uncultured
Pseudahrensia
Labrenzia
Filomicrobium
Cohaesibacter
Rhizobiales
NA
Yoonia−Loktanella
uncultured
Thalassobius
Shimia
Ruegeria
Roseobacter clade CHAB−I−5 lineage
Rhodobacteraceae
Pseudoruegeria
Phaeobacter
Limibaculum
HIMB11
Aliiroseovarius
Rhodobacterales
uncultured
AEGEAN−169 marine group
Rhodospirillales
Clade III
Clade Ia
SAR11 clade
SAR86 clade
SAR86 clade
NS11−12 marine group
Sphingobacteriales
Erythrobacter
Sphingomonadales
Staphylococcus
Staphylococcales
Woeseia
Steroidobacterales
Synechococcus CC9902
Cyanobium PCC−6307
Synechococcales
Rubritalea
Verrucomicrobiales
Vibrio
Photobacterium
Vibrionales
−10
0
10
20
AH vs DU (Log fold change)
0.00
0.25
0.50
0.75
1.00
Relative Abundance
Sample Type
Seawater
Mucus
Tissue Slurry
Tissue Slurry Skeleton
Sediment

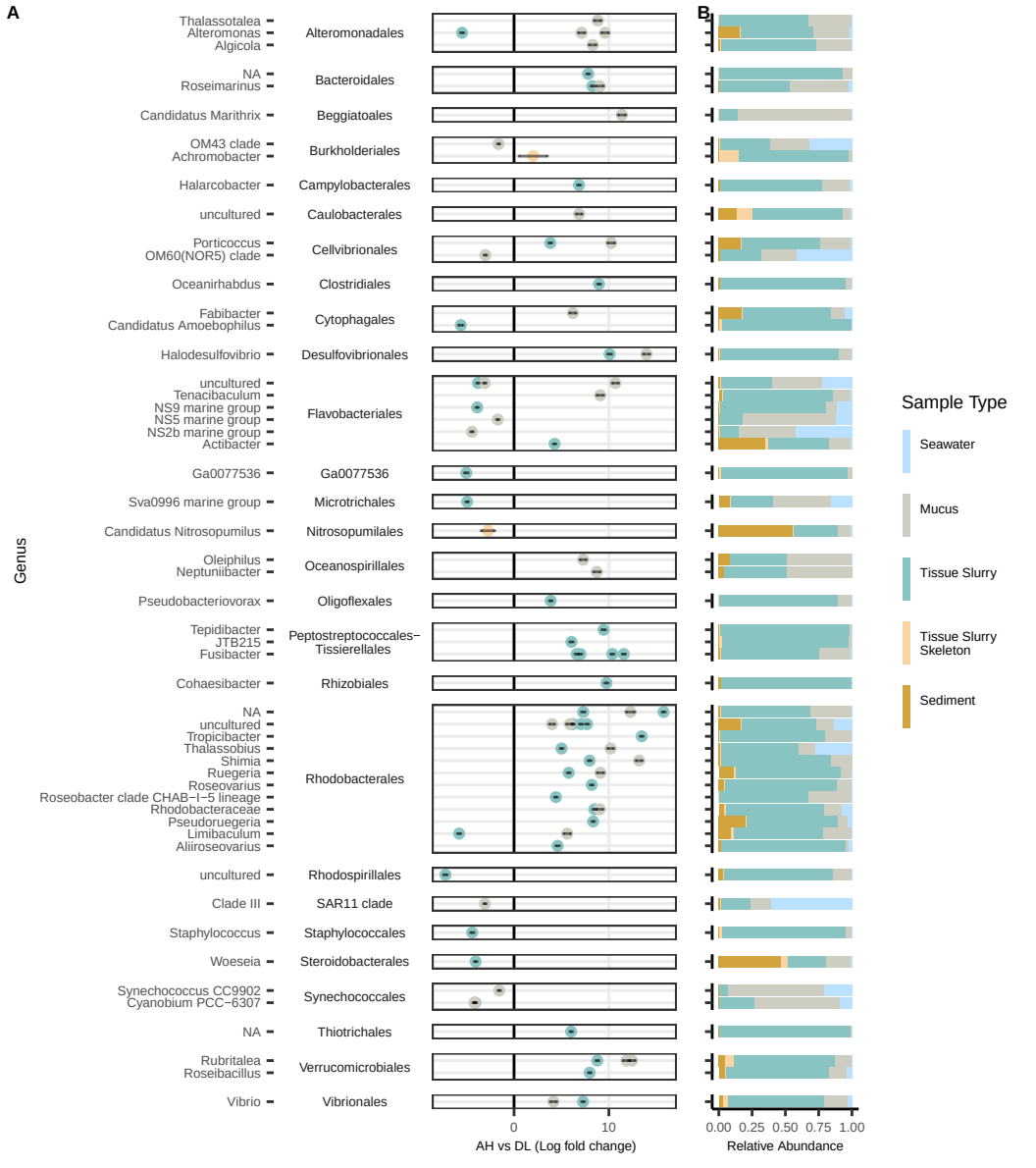
A
B
Genus
Thalassotalea
Alteromonas
Algicola
Alteromonadales
NA
Roseimarinus
Bacteroidales
Candidatus Marithrix
Beggiatoales
OM43 clade
Achromobacter
Burkholderiales
Halarcobacter
Campylobacterales
uncultured
Caulobacterales
Porticoccus
OM60(NOR5) clade
Cellvibrionales
Oceanirhabdus
Clostridiales
Fabibacter
Candidatus Amoebophilus
Cytophagales
Halodesulfovibrio
Desulfovibrionales
uncultured
Tenacibaculum
NS9 marine group
NS5 marine group
NS2b marine group
Actibacter
Flavobacteriales
Ga0077536
Ga0077536
Sva0996 marine group
Microtrichales
Candidatus Nitrosopumilus
Nitrosopumilales
Oleiphilus
Neptuniibacter
Oceanospirillales
Pseudobacteriovorax
Oligoflexales
Tepidibacter
JTB215
Fusibacter
Peptostreptococcales−
Tissierellales
Cohaesibacter
Rhizobiales
NA
uncultured
Tropicibacter
Thalassobius
Shimia
Ruegeria
Roseovarius
Roseobacter clade CHAB−I−5 lineage
Rhodobacteraceae
Pseudoruegeria
Limibaculum
Aliiroseovarius
Rhodobacterales
uncultured
Rhodospirillales
Clade III
SAR11 clade
Staphylococcus
Staphylococcales
Woeseia
Steroidobacterales
Synechococcus CC9902
Cyanobium PCC−6307
Synechococcales
NA
Thiotrichales
Rubritalea
Roseibacillus
Verrucomicrobiales
Vibrio
Vibrionales
0
10
AH vs DL (Log fold change)
0.00
0.25
0.50
0.75
1.00
Relative Abundance
Sample Type
Seawater
Mucus
Tissue Slurry
Tissue Slurry Skeleton
Sediment

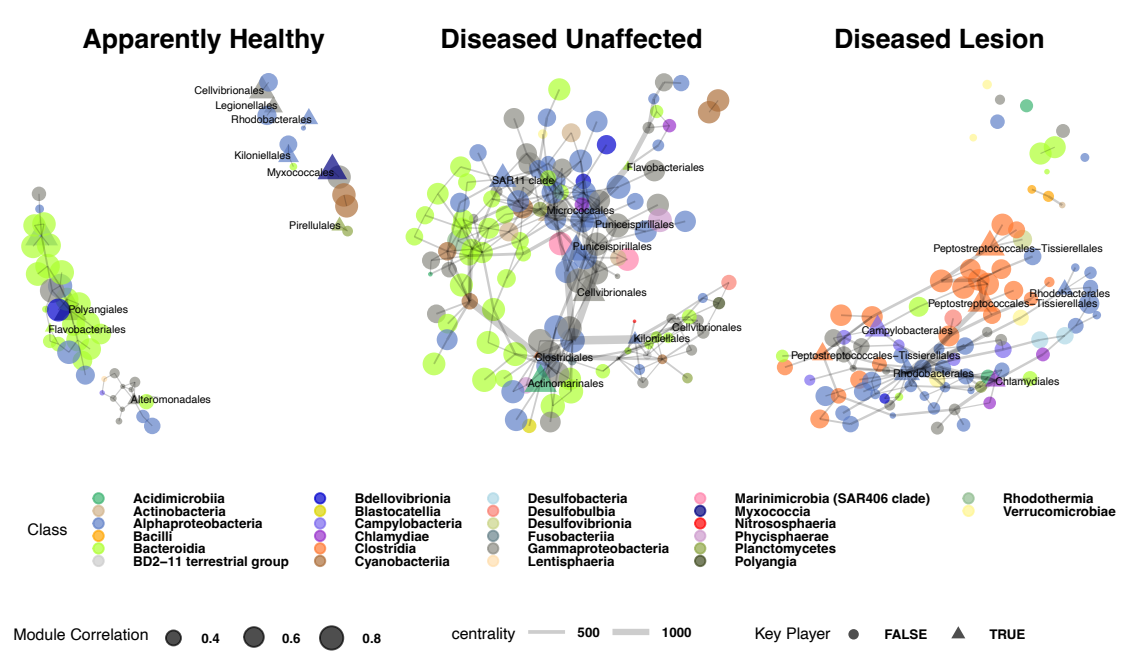
Apparently Healthy
Diseased Unaffected
Diseased Lesion
Cellvibrionales
Legionellales
Rhodobacterales
Kiloniellales
Myxococcales
Pirellulales
Polyangiales
Flavobacteriales
Alteromonadales
SAR11 clade
Flavobacteriales
Micrococcales
Puniceispirillales
Puniceispirillales
Cellvibrionales
Cellvibrionales
Kiloniellales
Clostridiales
Actinomarinales
Peptostreptococcales−Tissierellales
Rhodobacterales
Peptostreptococcales−Tissierellales
Campylobacterales
Peptostreptococcales−Tissierellales
Rhodobacterales
Chlamydiales
Class
Acidimicrobiia
Actinobacteria
Alphaproteobacteria
Bacilli
Bacteroidia
BD2−11 terrestrial group
Bdellovibrionia
Blastocatellia
Campylobacteria
Chlamydiae
Clostridia
Cyanobacteriia
Desulfobacteria
Desulfobulbia
Desulfovibrionia
Fusobacteriia
Gammaproteobacteria
Lentisphaeria
Marinimicrobia (SAR406 clade)
Myxococcia
Nitrososphaeria
Phycisphaerae
Planctomycetes
Polyangia
Rhodothermia
Verrucomicrobiae
Module Correlation
0.4
0.6
0.8
centrality
500
1000
Key Player
FALSE
TRUE